

Electronic Supplementary Information for MS:

**A series of porous interpenetrating metal-organic frameworks based
on fluorescent ligand for nitroaromatic explosives detection**

Xiao-Shan Zeng,^a Hui-Ling Xu,^a Yu-Ci Xu,^a Xiao-Qing Li,^a Zhao-Yang Nie,^a

Shu-Zhen Gao^a and Dong-Rong Xiao^{*ab}

^a College of Chemistry and Chemical Engineering, Southwest University, Chongqing, 400715, P. R. China

^b State Key Laboratory of Structural Chemistry, Fujian Institute of Research on the Structure of Matter, Chinese Academy of Sciences, Fuzhou, Fujian 350002, PR China

Table S1 Crystal data and structure refinements for compounds **1-4**.

Compound	1	2	3	4
Empirical formula	C ₈₁ H ₆₉ Cd ₂ Cl ₂ N ₁₄ O ₁₀	C ₃₉ H ₂₆ CdN ₆ O ₄ S	C ₄₃ H ₃₅ CdN ₇ O ₆	C ₁₆₈ H ₁₅₄ Cd ₅ Cl ₄ N ₃₀ O ₂₃
M _r (g mol ⁻¹)	1694.23	787.12	858.18	3665.03
Crystal system	Monoclinic	Monoclinic	Monoclinic	Monoclinic
Space group	P2 ₁ /n	P2 ₁ /c	P2 ₁ /c	P2 ₁ /n
a (Å)	21.0221(5)	10.5969(3)	10.1231(2)	21.0432(4)
b (Å)	17.4201(5)	14.7104(4)	14.8998(3)	17.4458(3)
c (Å)	26.3666(7)	28.7304(7)	28.9502(7)	26.3825(4)
α (°)	90	90	90	90
β (°)	111.047(3)	92.431(2)	94.192(2)	111.3592(19)
γ (°)	90	90	90	90
V (Å ³)	9011.5(4)	4474.59(19)	4354.93(16)	9020.2(3)
Z	4	4	4	2
ρ _{calcd} (g·cm ⁻³)	1.247	1.168	1.309	1.320
μ (mm ⁻¹)	4.806	4.671	4.448	5.485
F(000)	3444.0	1592.0	1752.0	3320.0
2θ range/°	6.88-134.158	8.352-134.126	8.528-134.146	7.196-134.152
Reflections collected	40496	19111	30686	81643
Unique data (R _{int})	16038(0.0511)	7990(0.0377)	7761(0.0417)	16113(0.0555)
GOF on F ²	1.070	1.046	1.189	1.050
R ₁ ^a /wR ₂ ^b [>2σ(I)]	0.0768/0.2166	0.0436/0.1153	0.0987/0.2466	0.0764/0.2152
R ₁ ^a /wR ₂ ^b (all data)	0.0853/0.2256	0.0495/0.1185	0.1072/0.2511	0.0852/0.2235

^a R₁ = $\sum ||F_0| - |F_C|| / \sum |F_0|$; ^b wR₂ = $\sum [w(F_0^2 - F_C^2)^2] / \sum [w(F_0^2)^2]^{1/2}$

Table S2 Selected bond lengths (\AA) and angles ($^\circ$) for **1-4**.

Compound 1			
Cd(1)-N(1)	2.281(5)	Cd(2)-N(4)#4	2.350(5)
Cd(1)-N(7)	2.314(5)	Cd(2)-N(6)	2.312(6)
Cd(1)-N(12)#1	2.371(6)	Cd(2)-N(10)	2.283(6)
Cd(1)-O(3)#2	2.621(5)	Cd(2)-Cl(1)	2.518(2)
Cd(1)-O(4)#2	2.295(4)	Cd(2)-O(1)	2.507(4)
Cd(1)-O(5)#3	2.220(4)	Cd(2)-O(2)	2.273(4)
N(1)-Cd(1)-N(7)	95.52(19)	Cl(1)-Cd(2)-O(1)	165.10(11)
N(1)-Cd(1)-N(12)#1	84.83(18)	N(4)#4-Cd(2)-Cl(1)	96.17(14)
N(1)-Cd(1)-O(3)#2	86.88(16)	N(4)#4-Cd(2)-O(1)	82.05(16)
N(1)-Cd(1)-O(4)#2	140.01(18)	N(6)-Cd(2)-Cl(1)	96.31(18)
N(7)-Cd(1)-N(12)#1	171.7(2)	N(6)-Cd(2)-N(4)#4	167.4(2)
N(7)-Cd(1)-O(3)#2	88.48(18)	N(6)-Cd(2)-O(1)	85.42(19)
N(12)#1-Cd(1)-O(3)#2	83.30(17)	N(10)-Cd(2)-Cl(1)	100.17(16)
O(4)#2-Cd(1)-N(7)	88.28(18)	N(10)-Cd(2)-N(4)#4	87.14(19)
O(4)#2-Cd(1)-N(12)#1	86.19(18)	N(10)-Cd(2)-N(6)	92.4(2)
O(4)#2-Cd(1)-O(3)#2	53.35(14)	N(10)-Cd(2)-O(1)	94.53(18)
O(5)#3-Cd(1)-N(1)	122.18(18)	O(2)-Cd(2)-Cl(1)	110.21(12)
O(5)#3-Cd(1)-N(7)	93.10(19)	O(2)-Cd(2)-N(4)#4	86.22(17)
O(5)#3-Cd(1)-N(12)#1	93.69(18)	O(2)-Cd(2)-N(6)	87.79(19)
O(5)#3-Cd(1)-O(3)#2	150.51(15)	O(2)-Cd(2)-N(10)	149.41(19)
O(5)#3-Cd(1)-O(4)#2	97.23(16)	O(2)-Cd(2)-O(1)	54.98(14)
Compound 2			
Cd(1)-N(1)	2.289(3)	Cd(1)-O(2)	2.620(3)
Cd(1)-N(4)#2	2.308(3)	Cd(1)-O(3)#1	2.348(3)
Cd(1)-N(6)#3	2.334(3)	Cd(1)-O(4)#1	2.590(3)
Cd(1)-O(1)	2.306(2)	N(1)-Cd(1)-N(4)#2	172.96(12)
N(1)-Cd(1)-N(6)#3	95.65(11)	N(6)#3-Cd(1)-O(3)#1	81.80(11)
N(1)-Cd(1)-O(1)	92.80(10)	N(6)#3-Cd(1)-O(4)#1	135.01(10)
N(1)-Cd(1)-O(2)	94.01(10)	O(1)-Cd(1)-N(4)#2	87.35(10)
N(1)-Cd(1)-O(3)#1	84.62(11)	O(1)-Cd(1)-N(6)#3	133.01(10)
N(1)-Cd(1)-O(4)#1	84.30(11)	O(1)-Cd(1)-O(2)	53.29(9)
N(4)#2-Cd(1)-N(6)#3	89.37(11)	O(1)-Cd(1)-O(3)#1	145.10(10)
N(4)#2-Cd(1)-O(2)	91.73(10)	O(1)-Cd(1)-O(4)#1	91.77(9)

N(4)#2-Cd(1)-O(3)#1	91.23(11)	O(3)#1-Cd(1)-O(2)	161.53(9)
N(4)#2-Cd(1)-O(4)#1	88.66(11)	O(3)#1-Cd(1)-O(4)#1	53.33(9)
N(6)#3-Cd(1)-O(2)	80.01(10)	O(4)#1-Cd(1)-O(2)	144.98(8)

Compound 3

Cd(1)-N(1)	2.302(8)	Cd(1)-O(2)	2.631(7)
Cd(1)-N(4)#3	2.294(8)	Cd(1)-O(4)#2	2.473(7)
Cd(1)-N(6)#4	2.314(8)	Cd(1)-O(5)#2	2.384(6)
Cd(1)-O(1)	2.296(6)	N(1)-Cd(1)-N(6)#4	87.8(3)
N(1)-Cd(1)-O(2)	90.0(2)	N(4)#3-Cd(1)-O(2)	91.2(2)
N(1)-Cd(1)-O(4)#2	92.2(3)	N(4)#3-Cd(1)-O(4)#2	87.1(2)
N(1)-Cd(1)-O(5)#2	91.5(2)	N(4)#3-Cd(1)-O(5)#2	86.9(2)
N(4)#3-Cd(1)-N(1)	178.3(3)	N(6)#4-Cd(1)-O(2)	81.5(2)
N(4)#3-Cd(1)-N(6)#4	93.5(3)	N(6)#4-Cd(1)-O(4)#2	82.6(2)
N(4)#3-Cd(1)-O(1)	91.4(3)	N(6)#4-Cd(1)-O(5)#2	137.1(2)
O(1)-Cd(1)-N(1)	88.3(3)	O(1)-Cd(1)-O(5)#2	88.8(2)
O(1)-Cd(1)-N(6)#4	134.0(3)	O(4)#2-Cd(1)-O(2)	163.8(2)
O(1)-Cd(1)-O(2)	52.7(2)	O(5)#2-Cd(1)-O(2)	141.4(2)
O(1)-Cd(1)-O(4)#2	143.4(2)	O(5)#2-Cd(1)-O(4)#2	54.6(2)

Compound 4

Cd(1)-N(1)	2.354(5)	Cd(2)-N(10)#4	2.322(5)
Cd(1)-N(4)#1	2.325(5)	Cd(2)-N(12)	2.359(5)
Cd(1)-N(7)	2.284(5)	Cd(2)-O(1)	2.519(4)
Cd(1)-O(3)#2	2.284(4)	Cd(2)-O(2)	2.282(4)
Cd(1)-O(4)#2	2.634(4)	Cd(3)-Cl(1)	2.658(2)
Cd(1)-O(5)#3	2.237(4)	Cd(3)-O(7)	2.517(7)
Cd(2)-Cl(1)	2.5152(19)	Cd(3)-O(8)	2.425(5)
Cd(2)-N(6)	2.274(6)	Cd(3)-O(9)	2.281(15)
Cd(3)-O(10)	2.392(5)	N(1)-Cd(1)-O(4)#2	83.57(16)
N(4)#1-Cd(1)-N(1)	171.99(18)	N(6)-Cd(2)-O(1)	94.37(17)
N(4)#1-Cd(1)-O(4)#2	88.56(16)	N(6)-Cd(2)-O(2)	149.13(17)
N(7)-Cd(1)-N(1)	85.45(18)	N(10)#4-Cd(2)-N(12)	167.4(2)
N(7)-Cd(1)-N(4)#1	95.55(17)	N(10)#4-Cd(2)-O(1)	85.89(17)
N(7)-Cd(1)-O(3)#2	138.66(17)	N(12)-Cd(2)-O(1)	81.56(16)
N(7)-Cd(1)-O(4)#2	86.13(16)	O(2)-Cd(2)-Cl(1)	110.93(12)
O(3)#2-Cd(1)-N(1)	85.54(17)	O(2)-Cd(2)-N(10)#4	87.51(18)

O(3)#2-Cd(1)-N(4)#1	88.51(16)	O(2)-Cd(2)-N(12)	86.29(17)
O(3)#2-Cd(1)-O(4)#2	52.78(14)	O(2)-Cd(2)-O(1)	54.82(13)
O(5)#3-Cd(1)-N(1)	93.80(17)	O(7)-Cd(3)-Cl(1)	88.32(17)
O(5)#3-Cd(1)-N(4)#1	92.24(16)	O(8)-Cd(3)-O(7)	94.4(2)
O(5)#3-Cd(1)-N(7)	123.85(17)	O(9)-Cd(3)-O(7)	172.5(4)
O(5)#3-Cd(1)-O(3)#2	96.95(15)	O(9)-Cd(3)-O(8)	86.3(4)
O(5)#3-Cd(1)-O(4)#2	149.71(14)	O(9)-Cd(3)-O(10)	97.0(4)
N(6)-Cd(2)-N(10)#4	92.6(2)	O(10)-Cd(3)-O(7)	88.1(2)
N(6)-Cd(2)-N(12)	87.11(18)	O(10)-Cd(3)-O(8)	131.4(2)
Cl(1)-Cd(2)-O(1)	165.42(11)	N(6)-Cd(2)-Cl(1)	99.69(15)
N(10)#4-Cd(2)-Cl(1)	97.22(17)	N(12)-Cd(2)-Cl(1)	95.26(14)
O(8)-Cd(3)-Cl(1)	119.74(14)	O(9)-Cd(3)-Cl(1)	84.9(3)
O(10)-Cd(3)-Cl(1)	108.81(17)		

Symmetry transformations used to generate equivalent atoms: for **1**: #1 -1+x, +y, +z. #2 +x, +y, 1+z. #3 1/2-x, -1/2+y, 3/2-z. #4 1+x, +y, +z. #5 +x, +y, -1+z. #6 1/2-x, 1/2+y, 3/2-z; for **2**: #1 1+x, +y, +z. #2 1+x, 3/2-y, -1/2+z. #3 -1+x, 1+y, +z. #4 -1+x, +y, +z. #5 1+x, 3/2-y, 1/2+z. #6 1+x, -1+y, +z; for **3**: #1 1+x, +y, +z. #2 -1+x, +y, +z. #3 -1+x, 3/2-y, -1/2+z. #4 +x, 1/2-y, -1/2+z. #5 1+x, 3/2-y, 1/2+z. #6 +x, 1/2-y, 1/2+z; for **4**: #1, 1+x, +y, +z; #2, 1+x, +y, 1+z; #3, 3/2-x, 1/2+y, 3/2-z; #4, -1+x, +y, +z; #5, -1+x, +y, -1+z; #6, 3/2-x, -1/2+y, 3/2-z.

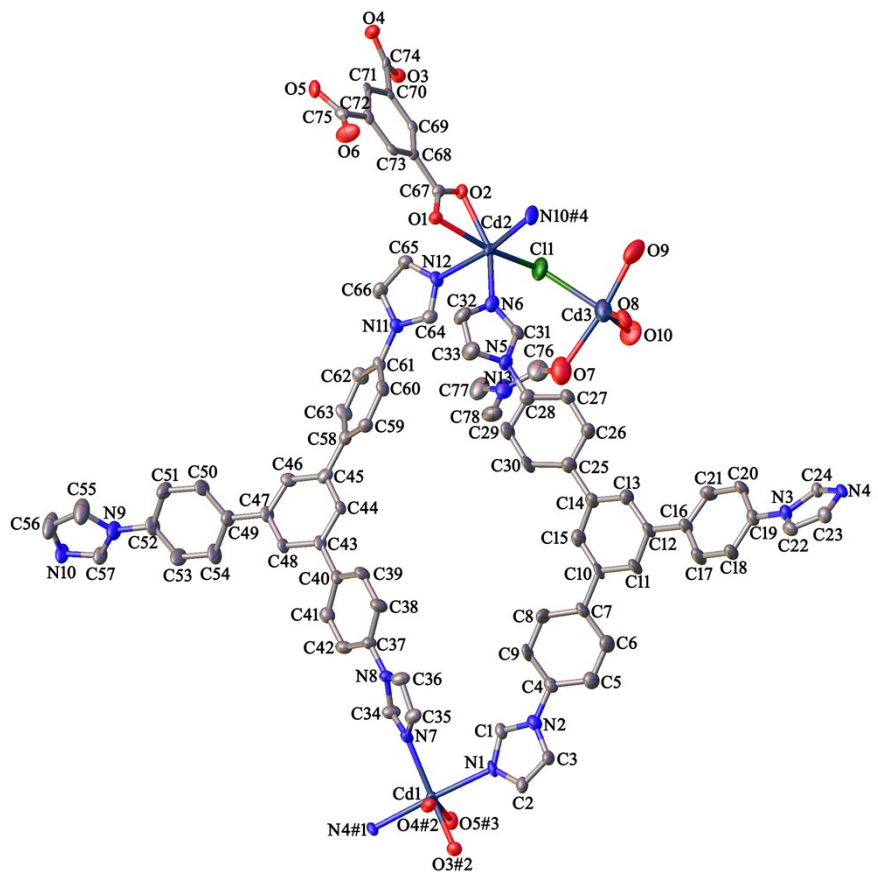


Fig. S1 The coordination environments of Cd atoms in compound 4.

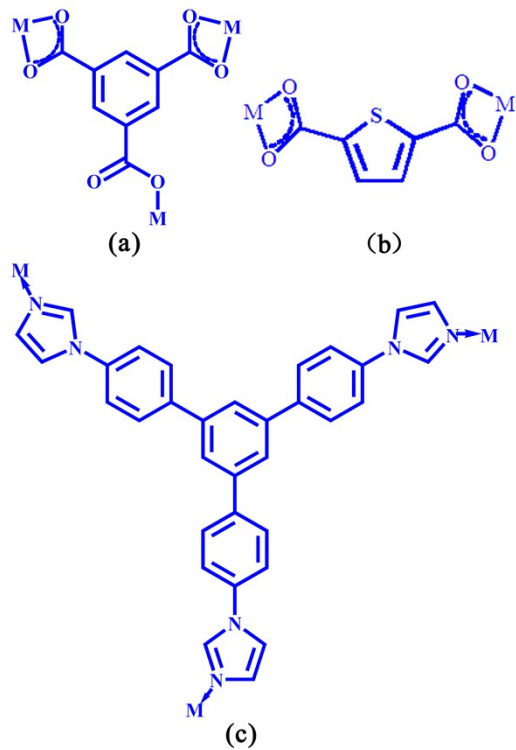


Fig. S2 The coordination mode of btc ligand (a), tdc ligand (b) and Tipb ligand (c).

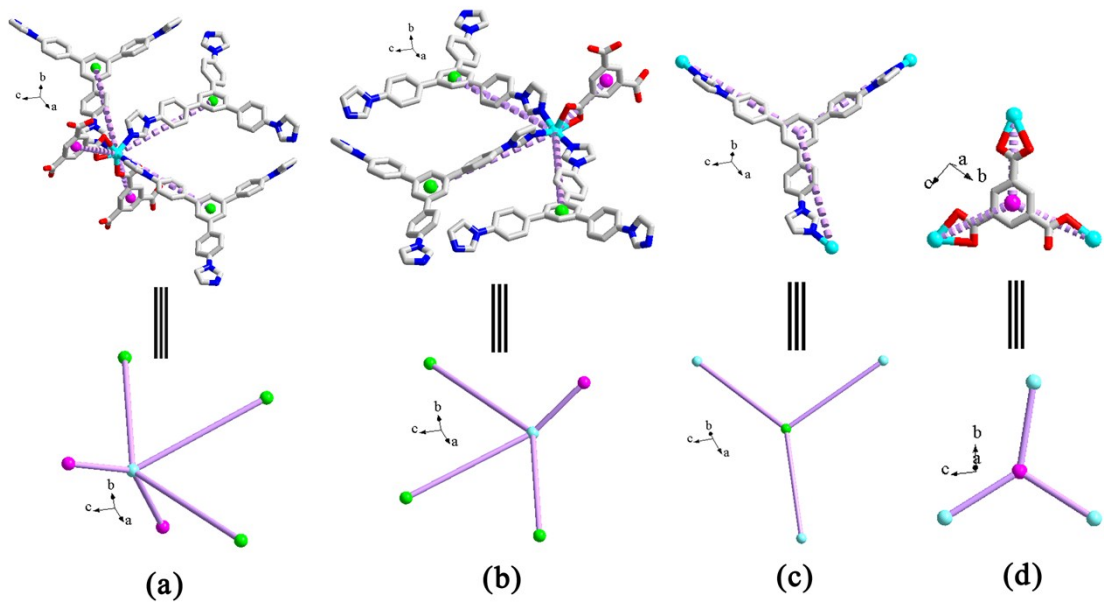


Fig. S3 Perspective view (upper) and simplified view (down) of Cd atoms, Tipb ligand and btc ligand in compound 1.

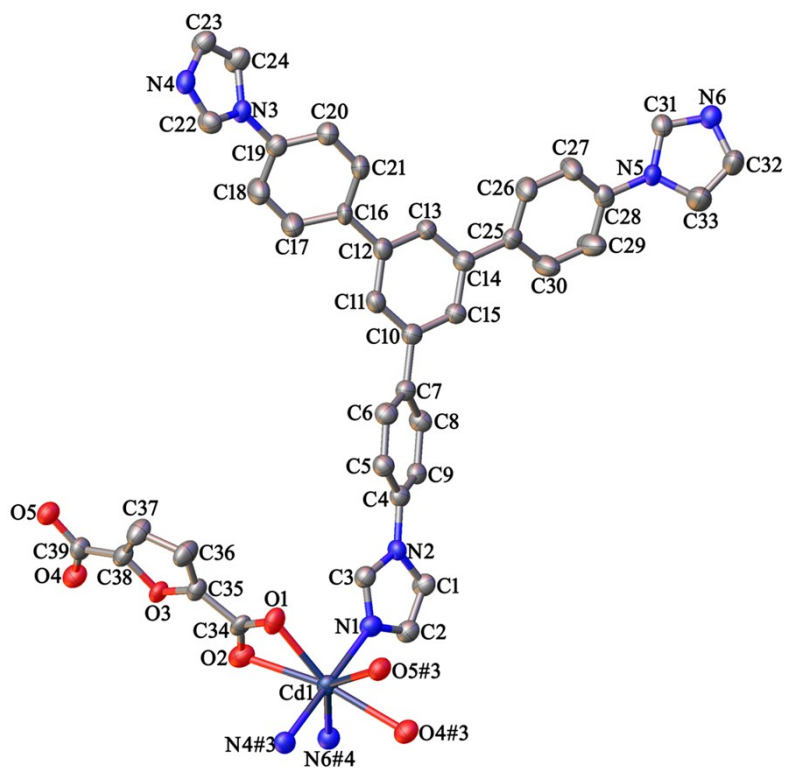


Fig. S4 The coordination environment of Cd atom in compound 3.

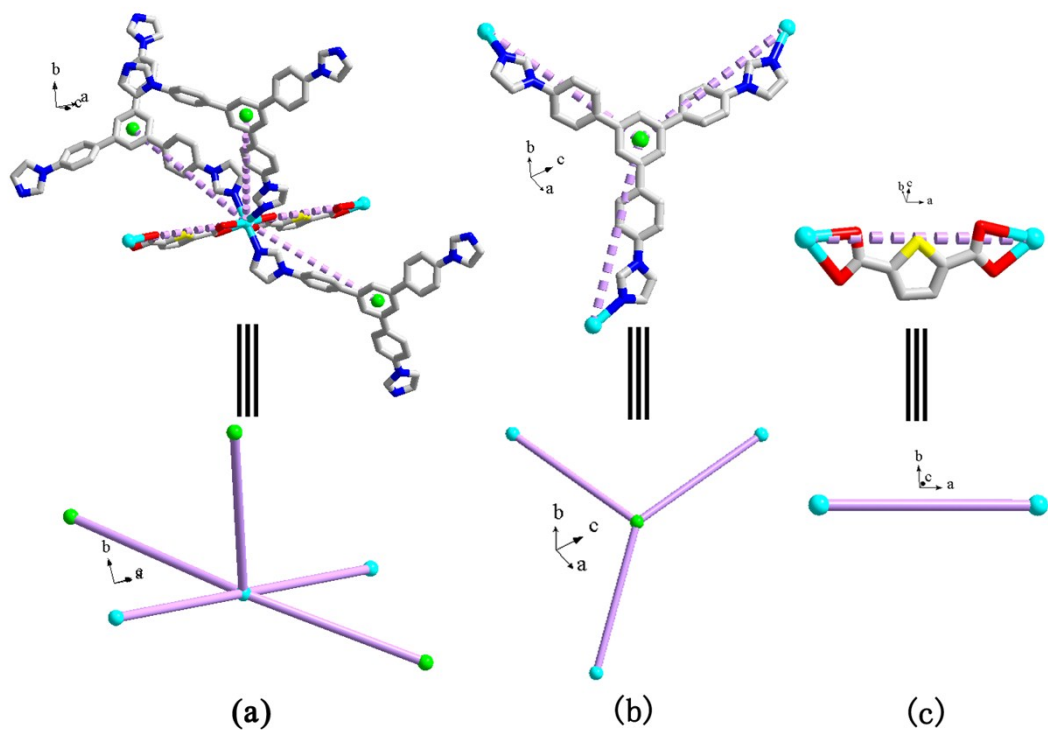


Fig. S5 Perspective view (upper) and simplified view (down) of the Cd atom, Tipb ligand and tdc linear linker in compound 2.

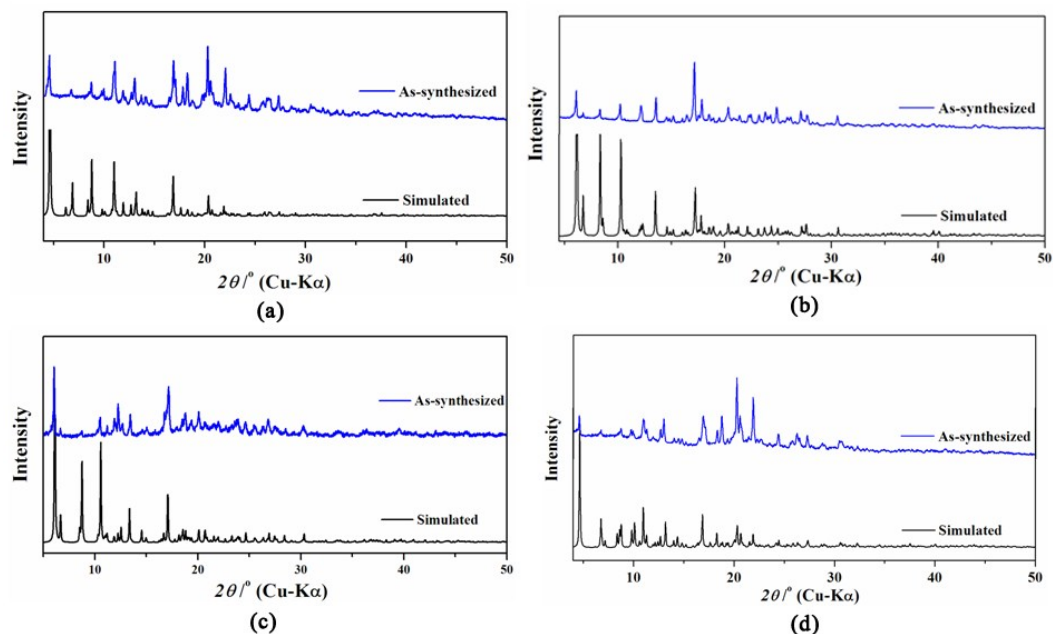


Fig. S6 The PXRD patterns of simulated and as-synthesized samples of compounds 1 (a), 2 (b), 3 (c), 4 (d).

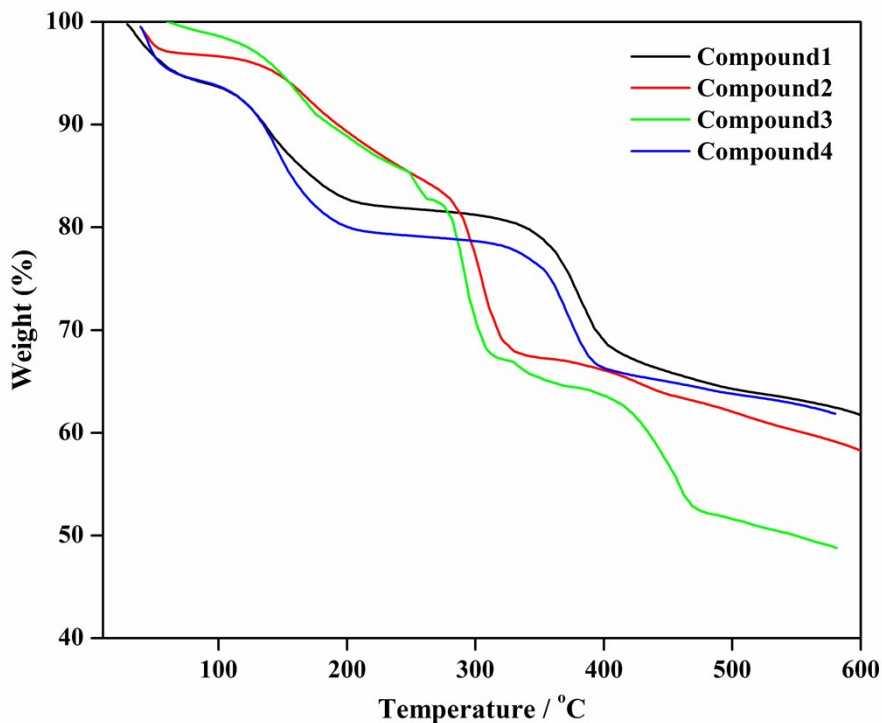


Fig. S7 The TG curves of compounds **1–4**.

The thermal stability of compounds **1–4** were examined using TGA in a nitrogen atmosphere. The TG curve (Fig. S7) of compound **1** shows a weight loss of 6.65% from room temperature to 105 °C, which corresponds to the loss of lattice DMF molecules. For compound **2**, the weight loss of 3.96% from room temperature to 126 °C is corresponding to DMA molecules. As depicted in Fig.S7, the TG curve of compound **3** displays weight loss of 2.36% from room temperature to 121 °C. For compound **4**, the weight loss of 6.65% from room temperature to 107 °C is assign to DMF molecules.

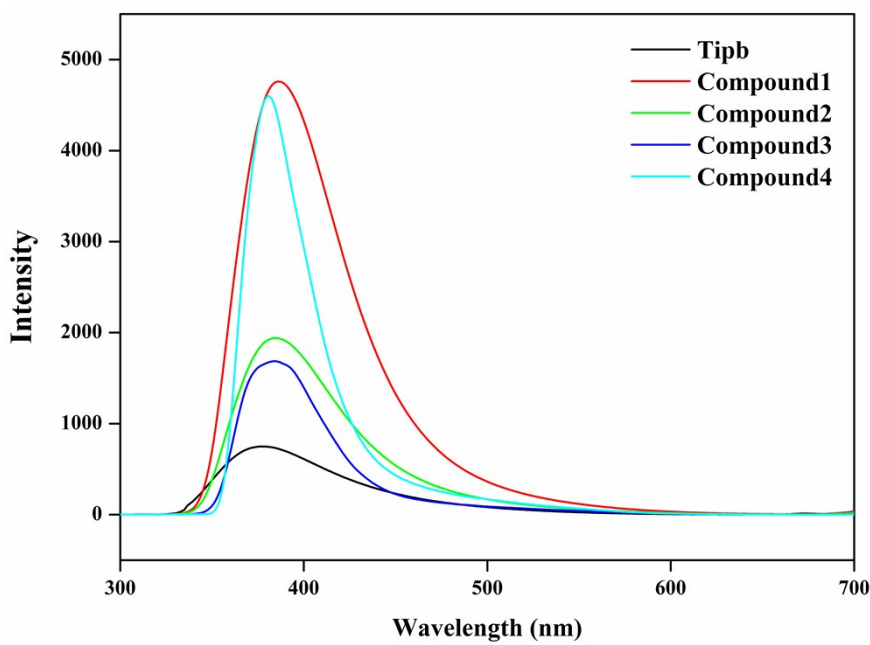


Fig. S8 Emission spectra of four compounds and Tipb ligand ($\lambda_{\text{ex}} = 278 \text{ nm}$) in the solid state at room temperature.

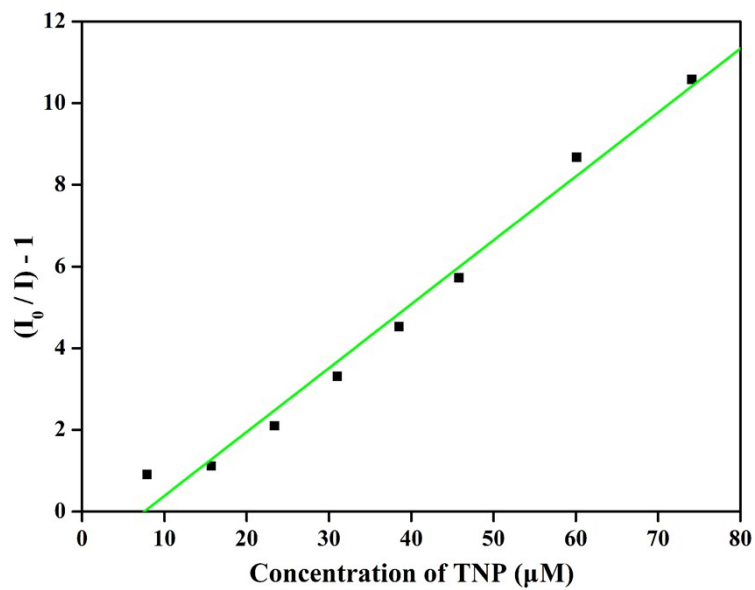


Fig. S9 Stern-Volmer plot of solid **1** dispersed in MeCN, and the fitted curve in the TNP concentration range of $0-74 \times 10^{-6} \text{ M}$.

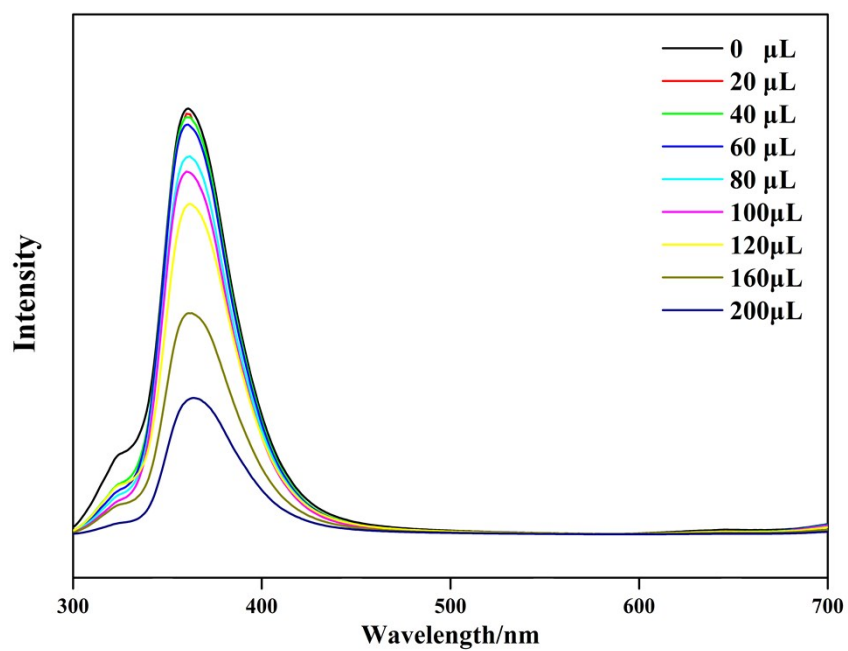


Fig. S10 Effect on the emission spectra of **1** dispersed in MeCN upon incremental addition of NB solution.

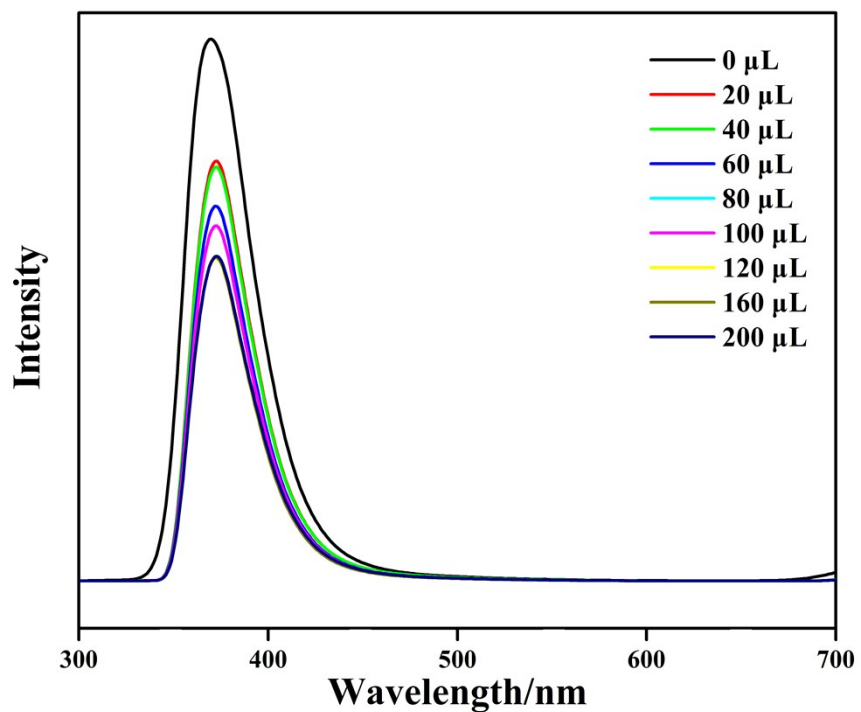


Fig. S11 Effect on the emission spectra of **1** dispersed in MeCN upon incremental addition of 2,4-DNT solution.

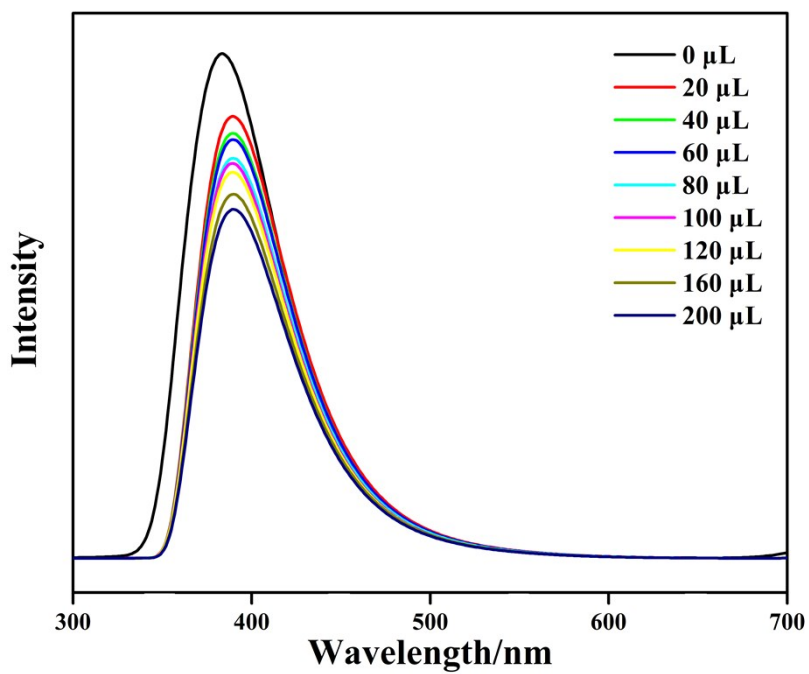


Fig. S12 Effect on the emission spectra of **1** dispersed in MeCN upon incremental addition of 1,3-DNB solution.

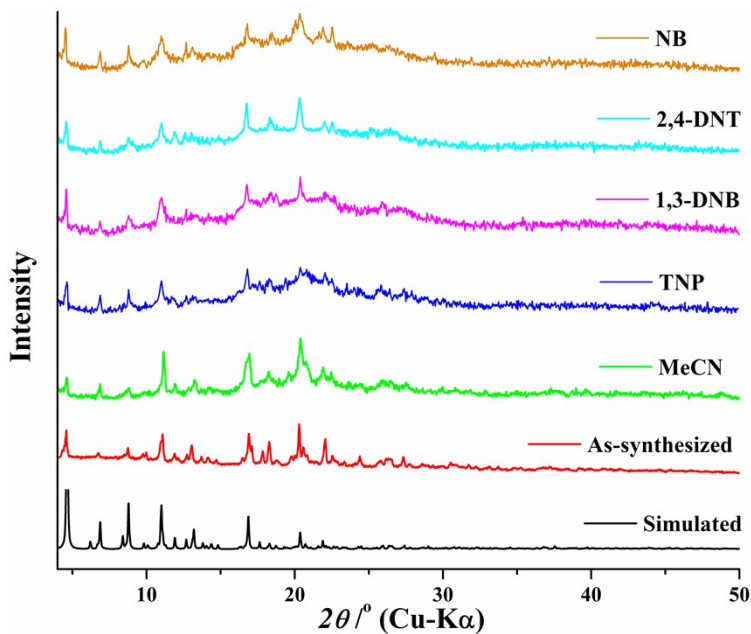


Fig. S13 The PXRD patterns of compound **1** in different forms: simulated (black); as-synthesized (red); dispersed in MeCN (green); after 5 cycles of fluorescence quenching experiments with different nitroaromatic explosives at 7.4×10^{-5} M concentration (TNP, blue; 1,3-DNB, magenta; 2,4-DNT, cyan; NB, brown).

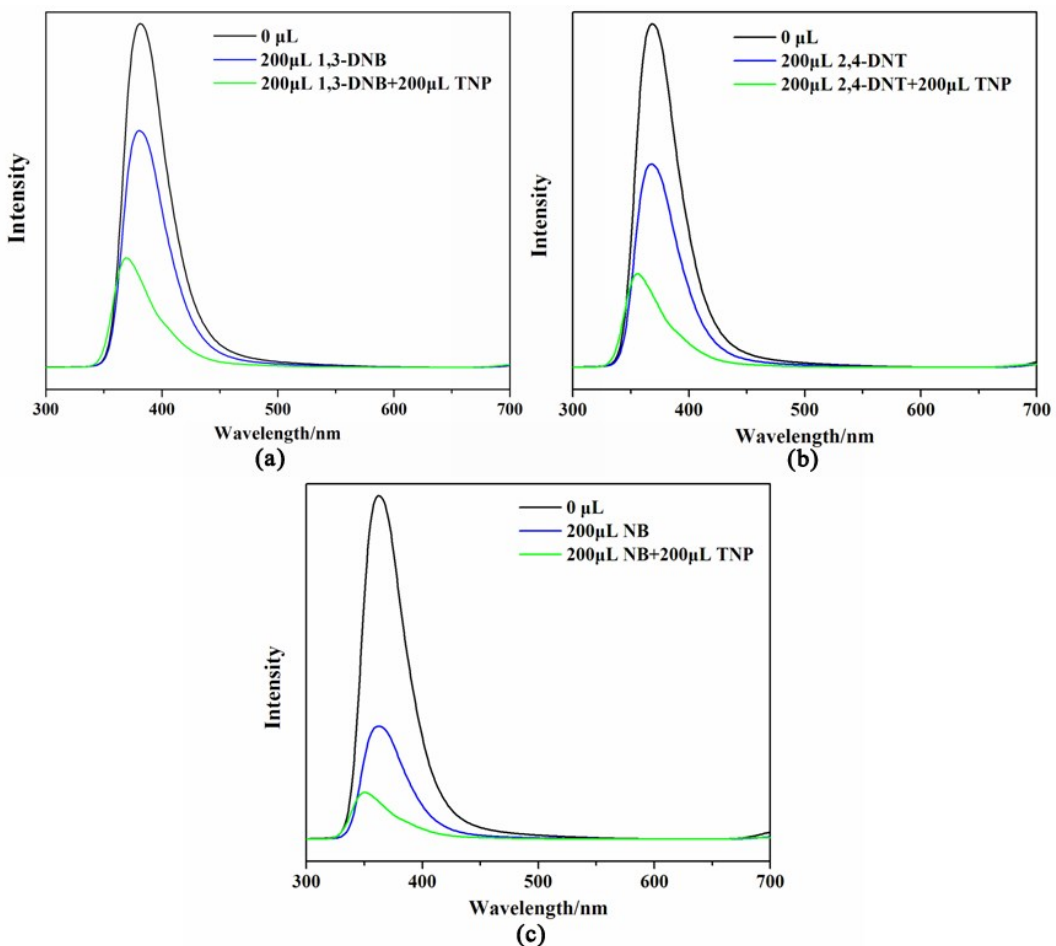


Fig. S14 Emission spectra of compound **1** dispersed in MeCN upon addition of 200 μL of 1 mM 1,3-DNB (a), 2,4-DNT (b), NB (c) solutions followed by 200 μL of 1 mM TNP solution.

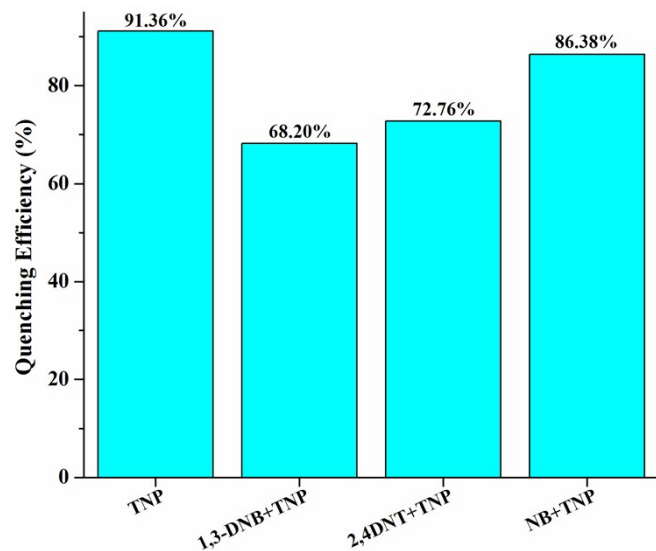


Fig. S15 Quenching efficiencies of TNP (6.9×10^{-5} M) in the presence of other nitroaromatic explosives (6.9×10^{-5} M) for compound **1**.

In order to investigate the selectivity of compound **1** for TNP detection, fluorescence titration experiments were performed by addition of TNP solution (1mM, 200 μ L) to the suspension of **1** containing other nitroaromatic explosive (7.4×10^{-5} M). The fluorescence intensity decreased (Fig. S14), and the quenching efficiency increased. However, the quenching efficiencies of TNP in the presence of other nitroaromatic explosives were lower than that of adding TNP solution to suspension only (Fig. S15). These results revealed the appreciable selectivity of compound **1** towards TNP detection in the presence of a higher concentration of other nitroaromatic explosive.

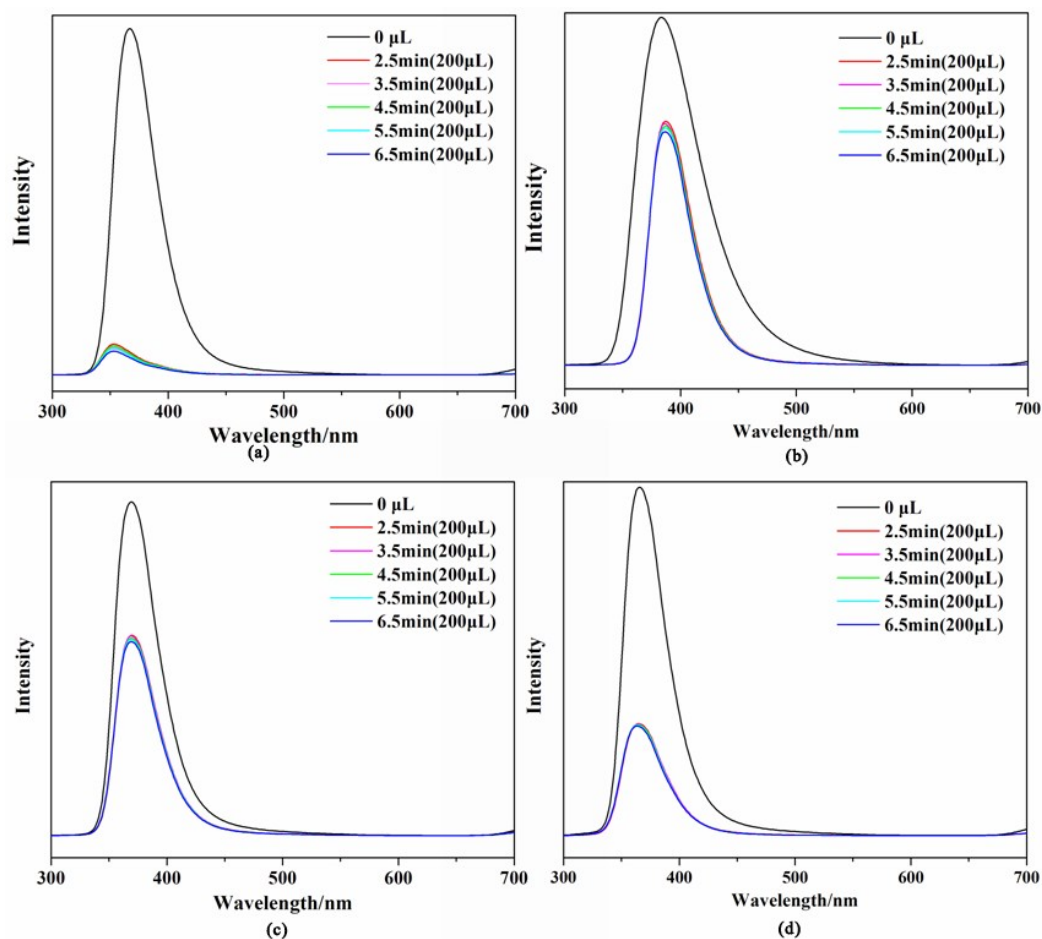


Fig. S16 Effect on emission spectra of compound **1** dispersed in MeCN upon addition of 200 μ L of 1 mM TNP (a), 1,3-DNB (b), 2,4-DNT (c), NB (d) solution in different exposure time.

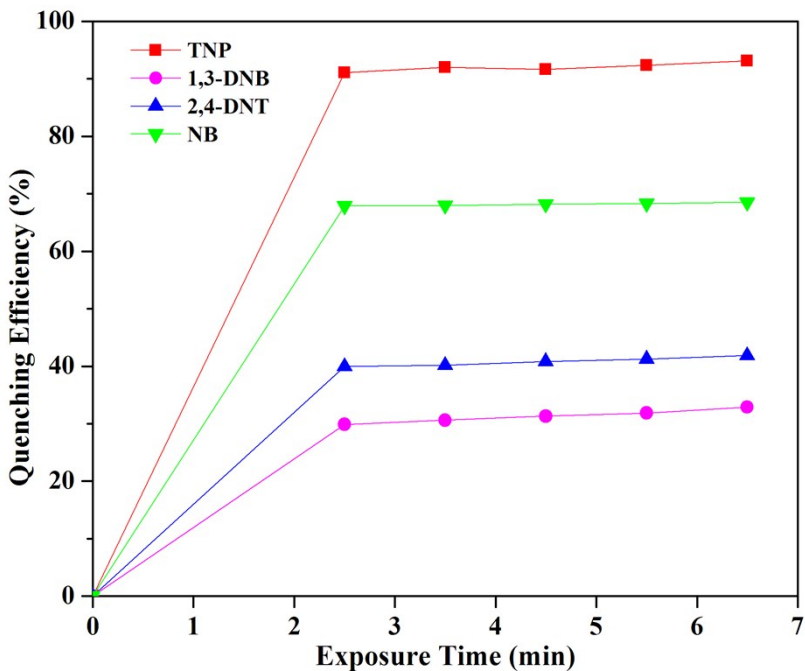


Fig. S17 Time-dependent fluorescence quenching by different nitroaromatic explosives (200 μ L of 1 mM explosives solution added to a 2.5 mL suspension of **1** in MeCN; TNP, red; 1,3-DNB, magenta; 2,4-DNT, blue; NB, viridescence).

In order to determine the response time for detection of explosives by **1**, time-dependent fluorescence quenching were measured in the presence of different nitroaromatic explosives (200 μ L of 1 mM explosives solution added to a 2.5 mL suspension of **1** in MeCN). The fluorescence intensity was measured at regular exposure time (Fig. S16). The plots of quenching efficiencies versus exposure time (Fig. S17) reveal that stable signal was obtained about 2.5 min.

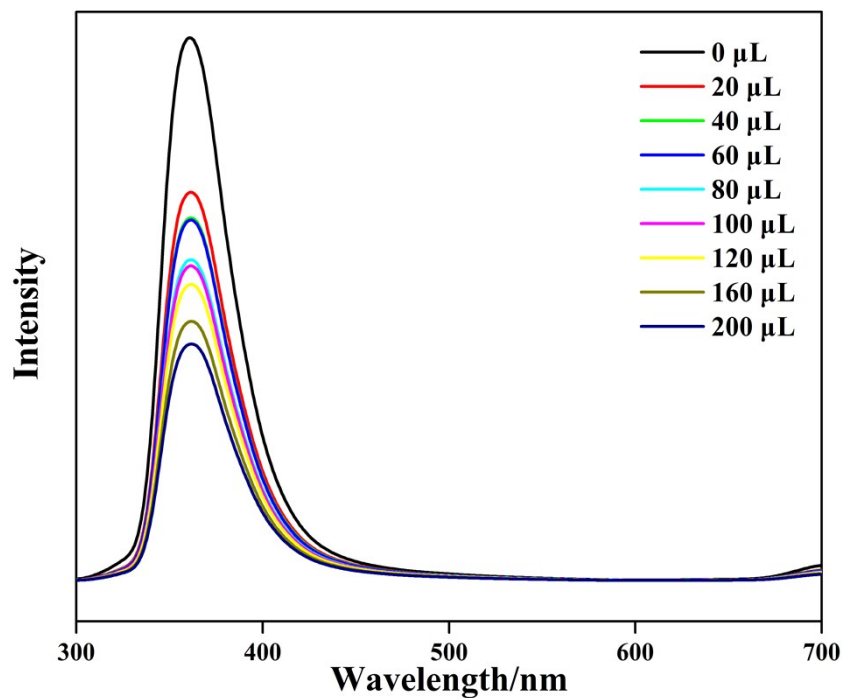


Fig. S18 Effect on the emission spectra of **2** dispersed in MeCN upon incremental addition of NB solution.

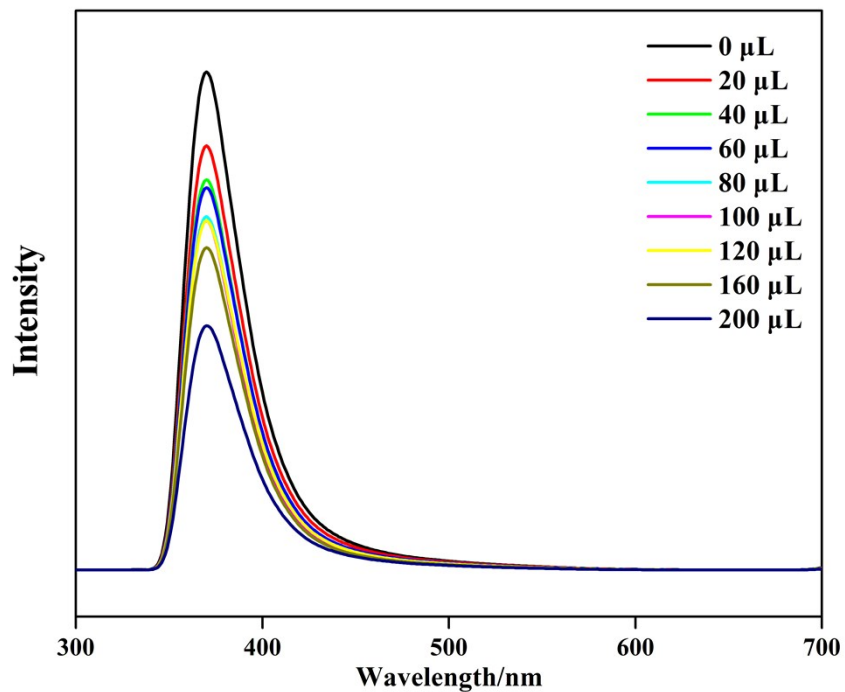


Fig. S19 Effect on the emission spectra of **2** dispersed in MeCN upon incremental addition of 2,4-DNT solution.

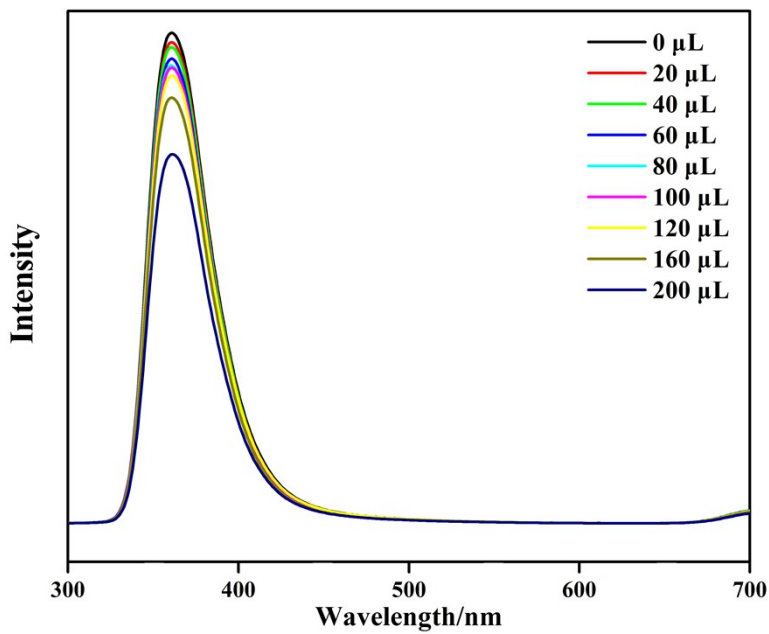


Fig. S20 Effect on the emission spectra of **2** dispersed in MeCN upon incremental addition of 1,3-DNB solution.

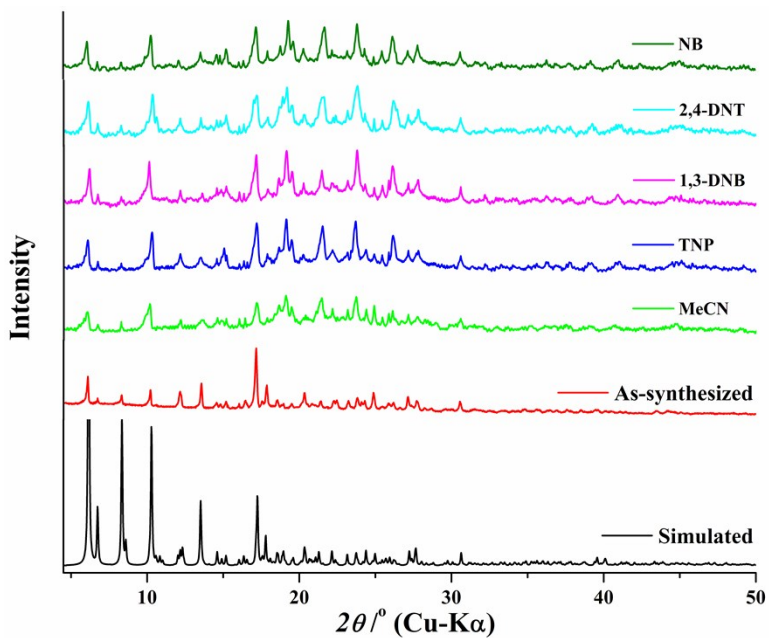


Fig. S21 The PXRD patterns of compound **2** in different forms: simulated (black); as-synthesized (red); dispersed in MeCN (viridescence); after 5 cycles of fluorescence quenching experiments with different nitroaromatic explosives at 7.4×10^{-5} M concentration (TNP, blue; 1,3-DNB, magenta; 2,4-DNT, cyan; NB, green).

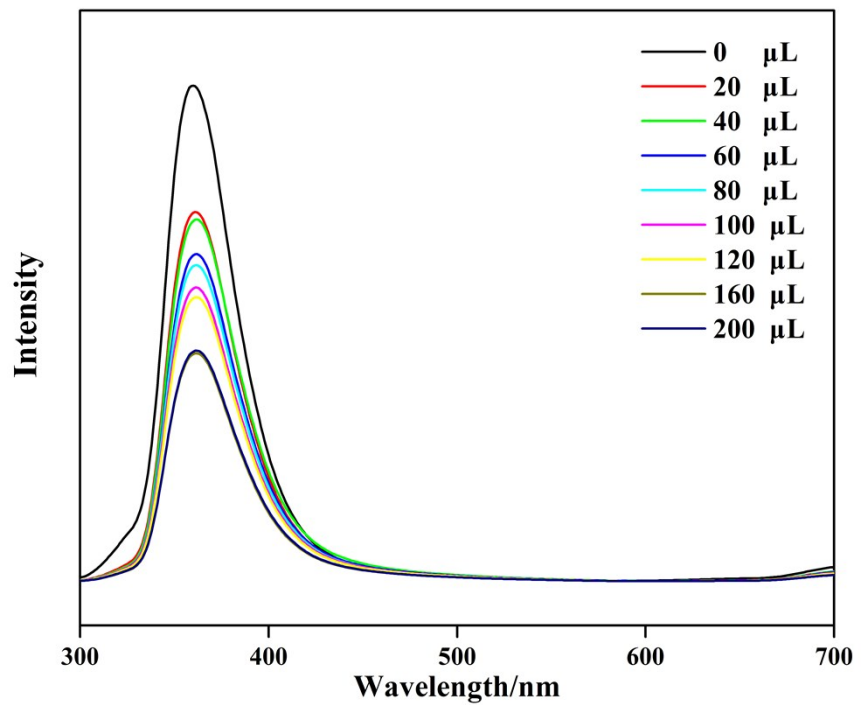


Fig. S22 Effect on the emission spectra of **3** dispersed in MeCN upon incremental addition of NB solution.

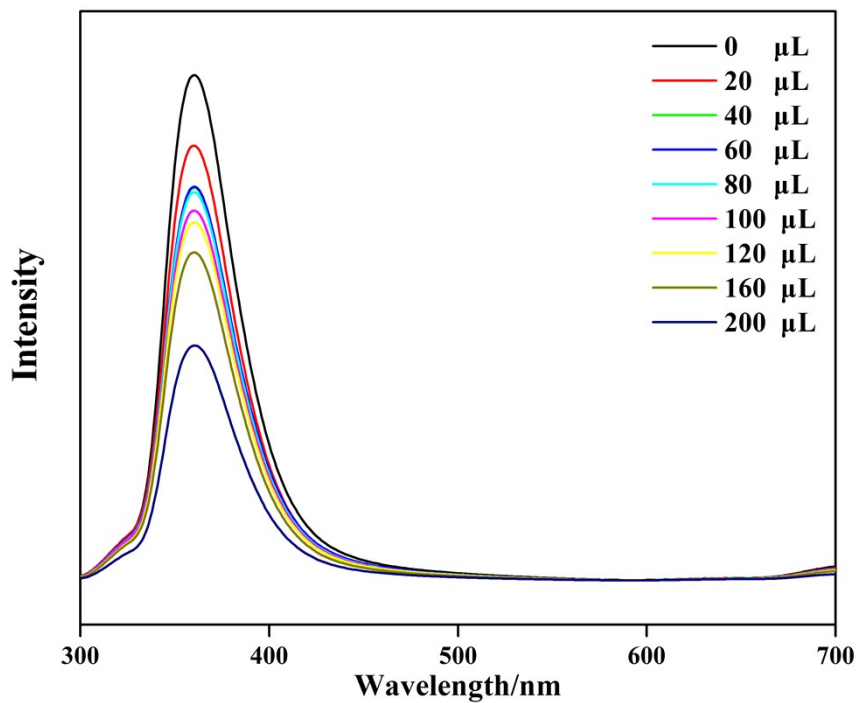


Fig. S23 Effect on the emission spectra of **3** dispersed in MeCN upon incremental addition of 2,4-DNT solution.

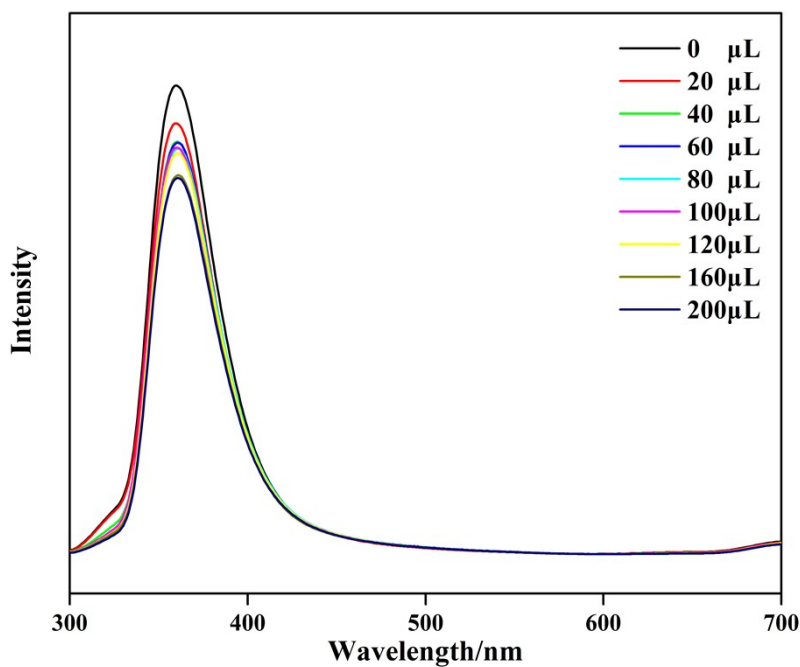


Fig. S24 Effect on the emission spectra of **3** dispersed in MeCN upon incremental addition of 1,3-DNB solution.

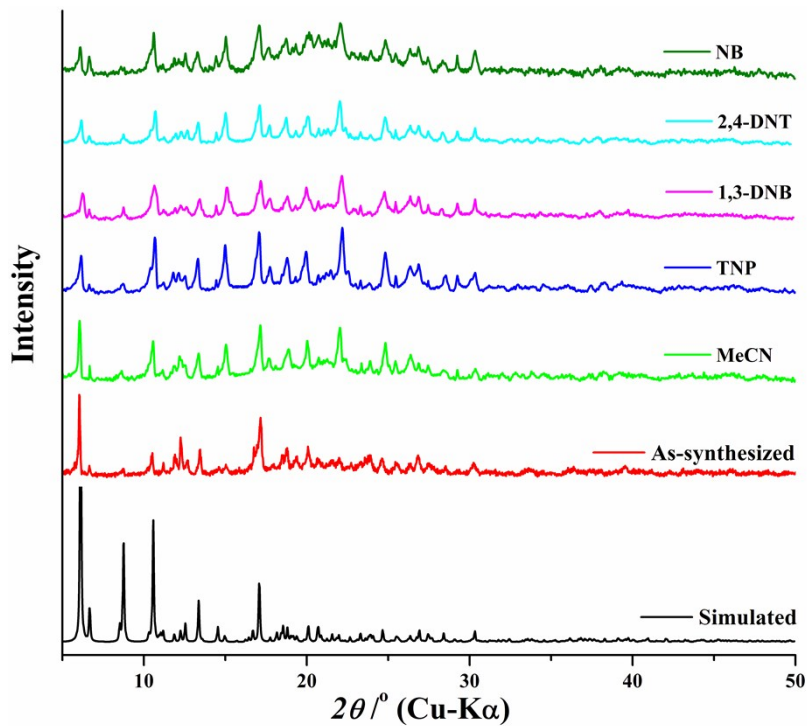


Fig. S25 The PXRD patterns of compound **3** in different forms: simulated (black); as-synthesized (red); dispersed in MeCN (viridescence); after 5 cycles of fluorescence quenching experiments with different nitroaromatic explosives at 7.4×10^{-5} M concentration (TNP, blue; 1,3-DNB, magenta; 2,4-DNT, cyan; NB, green).

Table S3. HOMO and LUMO energy levels of Tipb ligand and analytes calculated by density functional theory (DFT) at PBE0/6-31G* accuracy level using *Gaussian 16* package of programs.

Analytes	HOMO (eV)	LOMO (eV)	Band gap (eV)
Tipb	-6.2748	-1.6452	4.6296
TNP	-8.5073	-3.6966	4.8107
1,3-DNB	-8.7086	-2.9385	5.7701
2,4-DNT	-8.3843	-2.7913	5.5930
NB	-7.8882	-2.2147	5.6735

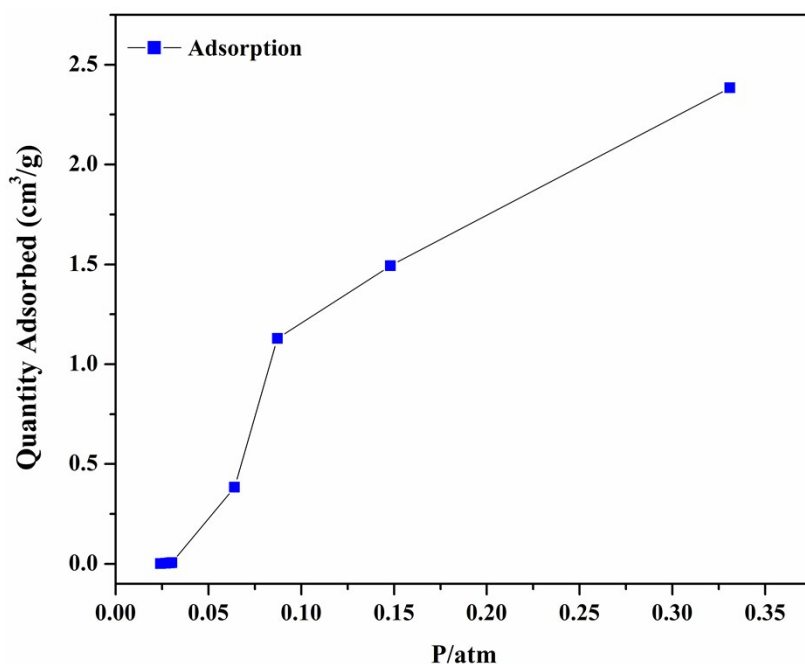


Fig. S26 N₂ sorption isotherms at 77 K of compound **1**.

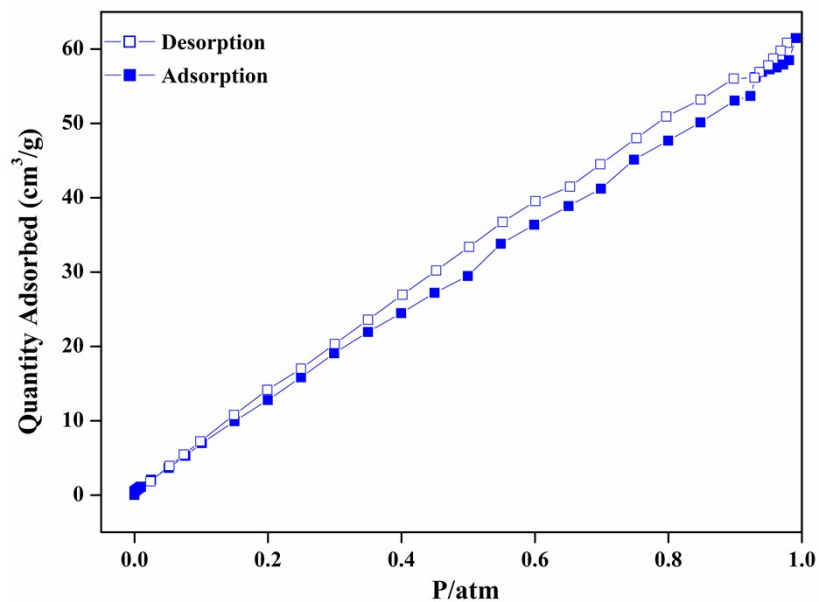


Fig. S27 N₂ sorption isotherms at 77 K of compound 2.

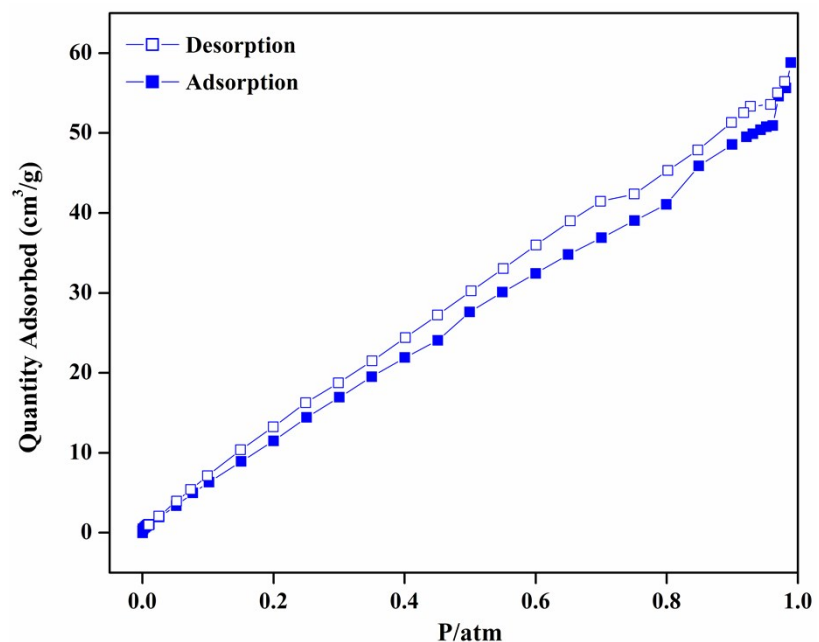


Fig. S28 N₂ sorption isotherms at 77 K of compound 3.

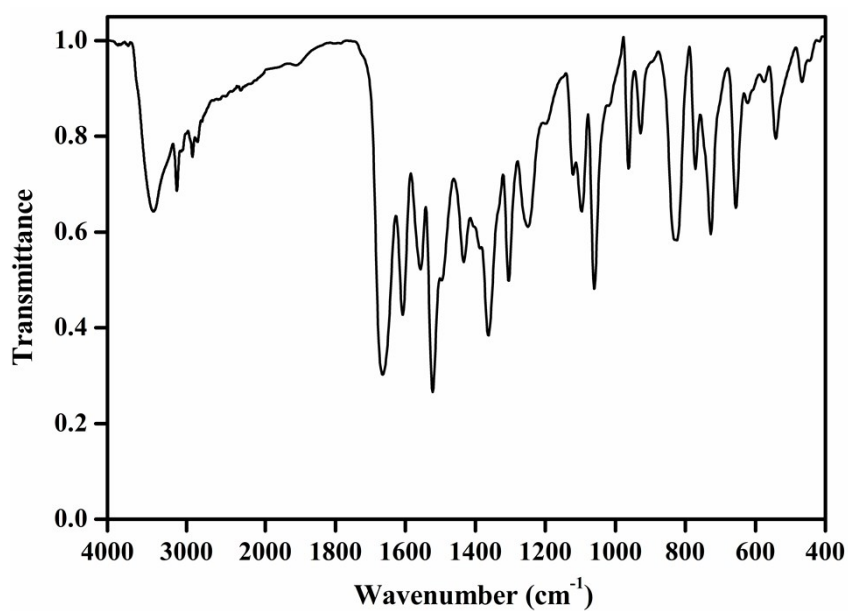


Fig. S29 IR spectra of compound **1**. FT/IR data (cm⁻¹): 3420(w), 3123(w), 2926(w), 2862(w), 2316(w), 1665(s), 1607(s), 1556(m), 1522(s), 1495(m), 1433(m), 1387(m), 1362(s), 1304(m), 1250(m), 1199(w), 1121(w), 1096(w), 1061(m), 1020(w), 962(w), 928(w), 826(m), 771(w), 727(m), 656(w), 623(w), 575(w), 542(w), 467(w), 446(w), 417(w).

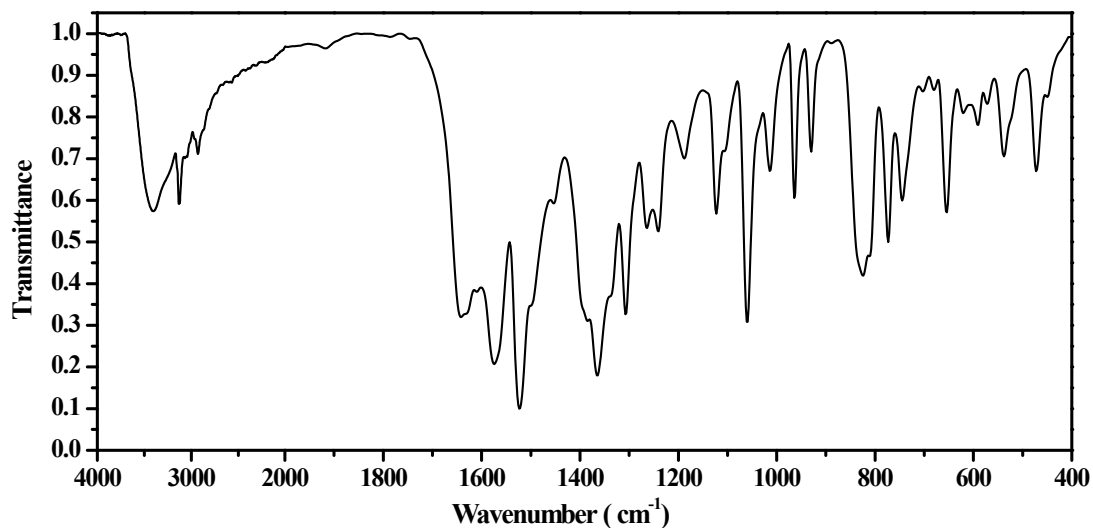


Fig. S30 IR spectra of compound **2**. FT/IR data (cm⁻¹): 3410(m), 3138(w), 2933(m), 1639(s), 1573(s), 1523(s), 1360(s), 1308(s), 1266(m), 1240(m), 1187(w), 1121(m), 1061(s), 1013(w), 964(w), 929(w), 827(m), 772(m), 743(w), 703(w), 670(w), 656(w), 622(w), 590(w), 572(w), 538(w), 515(w), and 469(w).

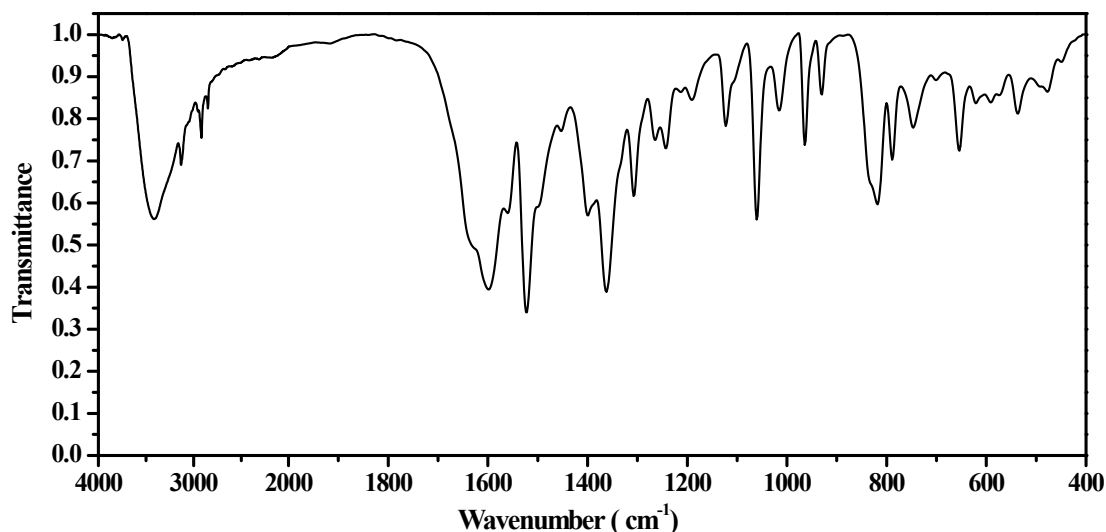


Fig. S31 IR spectra of compound 3. FT/IR data (cm⁻¹): 3414(m), 3124(w), 2918(w), 2851(w), 1599(s), 1559(m), 1523(s), 1452(w), 1400(m), 1363(s), 1305(s), 1266(w), 1242(w), 1213(w), 1190(w), 1124(w), 1061(m), 1013(s), 964(w), 930(w), 819(w), 787(w), 745(w), 701(w), 655(w), 619(w), 590(w), 535(w), 475(w).

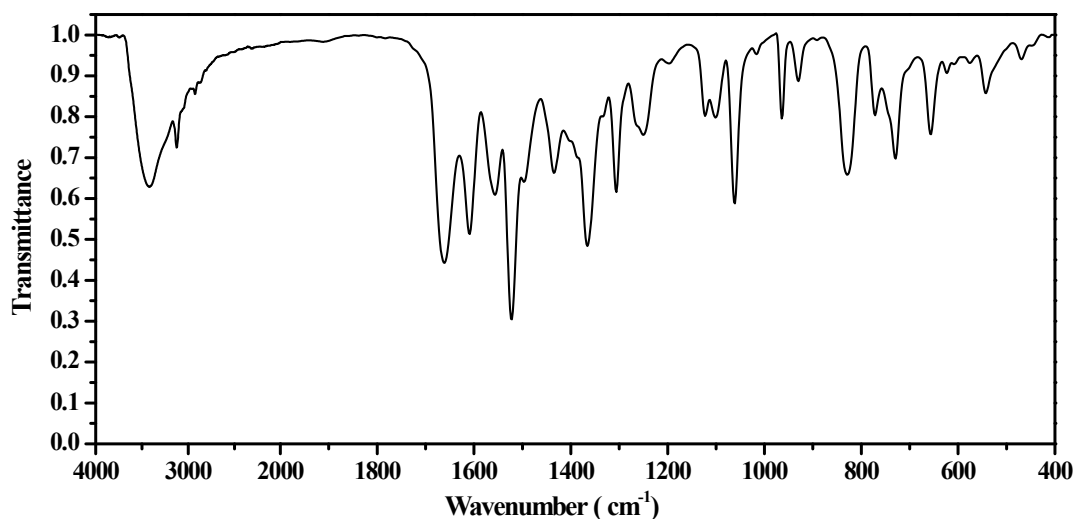


Fig. S32 IR spectra of compound 4. FT/IR data (cm⁻¹): 3426(w), 3124(w), 2933(w), 1663(s), 1610(m), 1558(w), 1523(s), 1494(w), 1434(w), 1366(m), 1305(w), 1250(w), 1198(w), 1124(w), 1099(w), 1061(w), 1016(w), 963(w), 929(w), 829(w), 772(w), 730(w), 656(w), 622(w), 575(w), 543(w), 470(w).